Analysis and diagnostics of the ECMWF model during ASTEX

E. Klinker (ECMWF)

1. Introduction

Experience at ECMWF in the last few years has shown that changes to the parametrization of planetary boundary layer processes had a noticeable impact on the quality of forecasts in the medium range. Modifications in various schemes improved the prediction of near surface parameters, which are increasingly used by operational forecasters. The quality of surface temperatures over land depends very much on how well the model predicts cloud cover. At ECMWF underestimation of cloud cover over land has led to a warm surface temperature bias in the summer and a cold bias in the winter. Maritime low level clouds have been a problem for some time and errors have affected coastal areas as well. Overestimation of clouds on low level inversions indicated shortcomings of the diagnostic cloud scheme.

The cloud fields in the ECMWF scheme (*Slingo*, 1987) are linked to large scale properties like relative humidity, vertical velocity and static stability. Schemes like this are widely used because of their simplicity and relative success in simulating quite well most types of clouds. However, the decoupling of diagnostic cloud schemes from the hydrological cycle limits the improvement that can be gained from future modifications. A better representation of cloud related processes can be achieved in a scheme in which the cloud properties are treated as prognostic parameters. The prognostic cloud scheme that is currently developed at ECMWF (*Tiedke*, 1993), defines the time evolution of clouds from the large-scale budget equations of cloud water content and cloud air.

Validation of model clouds from presently used schemes in operational forecasts or from cloud schemes under development is a difficult task due to a lack of sufficient validation data. Observational estimates derived from mainly infrared satellite measurements like those produced for the International Climatology Project (ISCCP, *Rossow and Schiffe*r, 1991) are useful for the validation of total cloud cover. However, for low level clouds the overlapping of higher level clouds limits the usage of the ISCCP clouds to a cloud cover estimate that represents only a lower limit. Synoptic observations are used for a continuous validation of operational products, where biases are possible from errors of subjective estimates. Field experiments like ASTEX deliver a welcome source of additional cloud information that will help to validate certain aspects of cloud cover.

The simulation of maritime stratocumulus with the present diagnostic cloud scheme and with the future prognostic scheme is closely linked to the ability of the model to retain a realistic structure of the boundary layer. The additional soundings available from the ASTEX experiments constitute an extensive data set that can be used to validate the structure of the PBL. A large portion of these observations were distributed via the GTS and have been used in the ECMWF assimilation. Other measurements were made available later and can serve as independent quality control in areas away from usual data sources.

Apart from the operational data assimilation products during the ASTEX campaign period, further 3-dimensional fields of diabatic and adiabatic tendencies were extracted from short range integrations which were run using a lower resolution of T106 compared to the T213 resolution of the operational model. These forecasts were run four times per day form the operational analysis of 0, 6, 12, and 18Z. With a forecast length of 7 hours and archiving frequency of one hour, a high resolution data set in time of all relevant physical processes has been generated.

For the validation of the forecasts large scale analyses are the most frequently used reference. Therefore the performance of the data assimilation system is discussed first in the next section. Short range forecast errors are then investigated in section 3 in the framework of a budget analysis of physical processes of temperature and humidity. This is followed by a discussion of the performance of the medium range forecast and a summary.

2. The performance of the ECMWF data assimilation system during ASTEX

The quality of the analysis depends to a large extent on the data density. Therefore the additional soundings in the ASTEX triangular which have been distributed via the GTS has helped to a better definition of the large scale flow in the analysis. The performance of the system can be measured in terms of root mean square errors (RMS-errors) and biases of the analysis compared to soundings. Fig. 1 shows a comparison of the data assimilation statistics between June 1992 and June 1991 for the two wind components, temperature and relative humidity. RMS-errors and the biases are calculated from departures of the radiosonde sounding

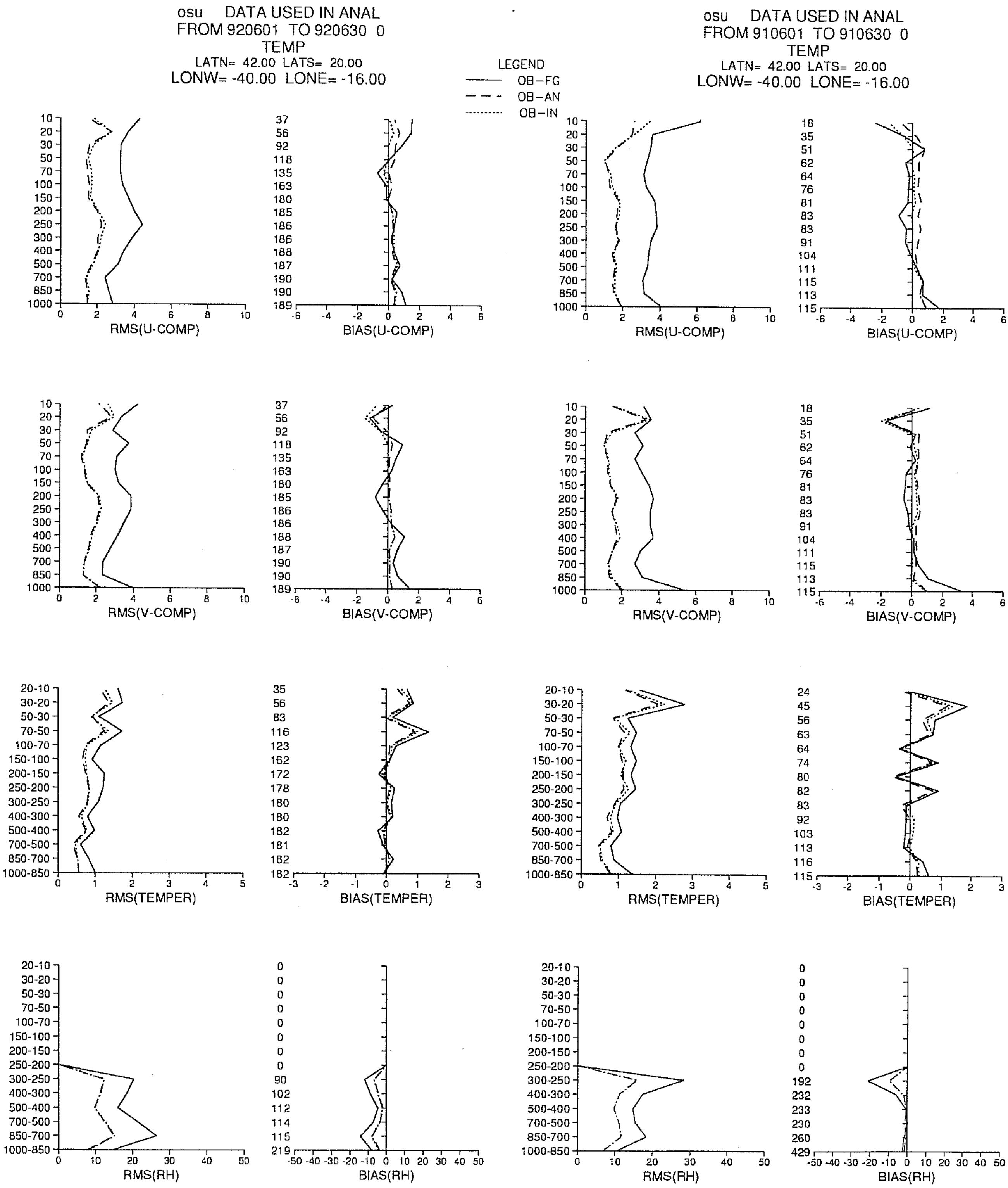

Fig. 1: Root-Mean-Square (RMS) differences and biases (BIAS) between observations and first Guess (FG), analysis (AN) and initialized analysis (IN) for the u- and v-component of the wind (upper two panels), temperature (third panel) and relative humidity (bottom panel). (a) June 1992, (b) June 1991.

from the back ground field (First guess=FG), the analysis (AN) and the initialized analysis (IN).

From the comparison it is obvious that a large number of additional ASTEX observations have been used in the ECMWF data assimilation system. The number of observations in June 1992 (shown between the BIAS- and the RMS-plot) is roughly up by a factor of two compared to June 1991. However, the RMS-errors of the wind components (top two panels) are not very different in the two years. Though the RMS-errors of the first guess at lower levels are improved in 1992, RMS-errors of the analysis and the initialized analysis are almost identical in June 1992 and 1991. The bias plots show a mixed picture for the performance of the first guess, whereas the analysis biases are generally reduced in June 1992.

A noticeably improved analysis can be seen for the temperature. RMS-errors of the first guess and the analysis are reduced in June 1992 at almost all levels and the bias-plot shows a much improved vertical structure of systematic errors, which is partly due to an increased vertical resolution of the model version used in June 1992 compared to June 1991. However, there are still systematic differences between observations and six-hour forecasts. The model bias indicates too low forecast temperatures in the layer 850 to 700 hPa and too low values between 700 and 400 hPa. A mixed picture emerges from the relative humidity statistics. RMS-errors at low levels have been reduced, whereas the fit to data is noticeably worse at upper levels in June 1992.

The results shown here are valid for the analysis time of 0Z, similar results can be seen for 12Z. In June 1992 the data-assimilation had a further benefit from additional soundings for 6Z and 18Z (app. 70 soundings for each time), which were totally absent in June 1991.

Fig.2 shows a comparison of a radiosonde sounding and a model profile for temperature and dew-point temperature for Porto Santo, where one of the observation sites was located during ASTEX. The strong low level temperature inversion at the top of the boundary layer is quite well kept by the analysis though the inversion top is slightly shifted upwards. This is probably the effect of the first guess, as a known systematic error of the model is to push the inversion height upward. The analysis has been less successful in representing the vertical structure of humidity. Particularly the sharp gradient at the inversion is smeared out in the vertical.

3. Budget analysis of temperature and humidity

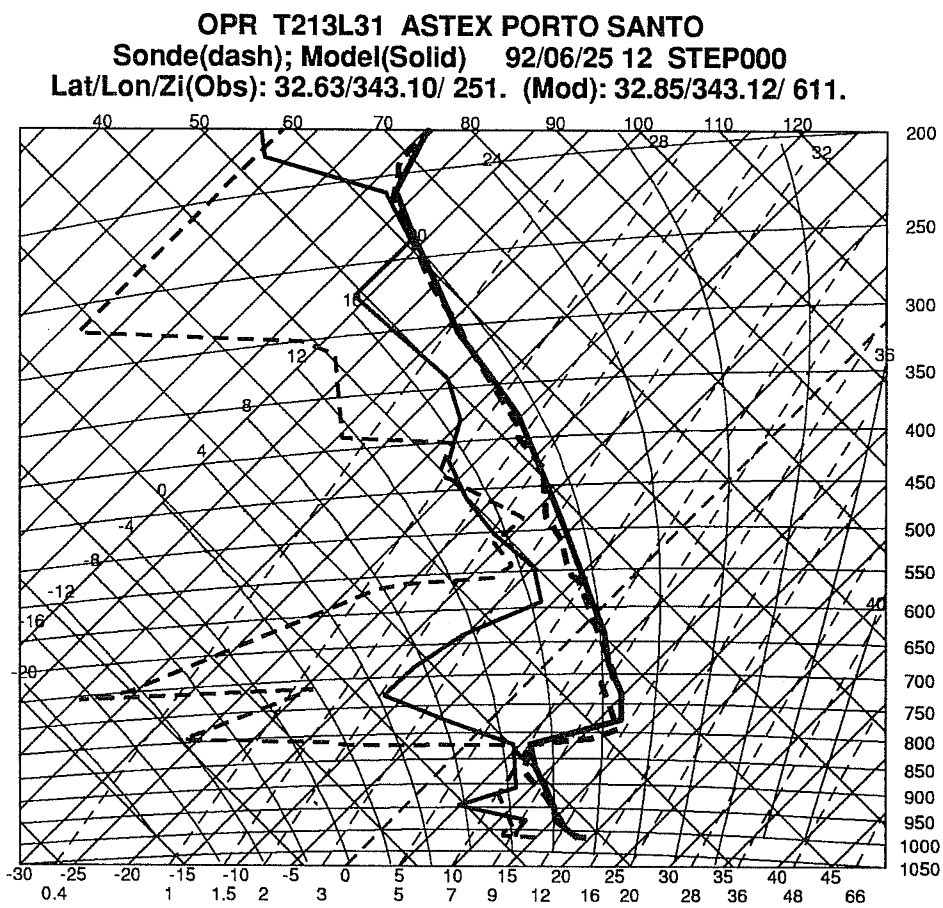

Fig. 2: Tephigram of temperature and dewpoint for 25 June 1992 at Porto Santo. Model values are drawn as solid lines, rawind sonde observations are drawn as dashed lines.

The short range forecasts performed during the ASTEX period of June 1992 have been used to investigate the budget of temperature and humidity. From the adiabatic tendencies of the model the required forcing to close the temperature and humidity budget can be calculated. This indirectly derived forcing is then compared to the diabatic forcing produced by the model's parametrization scheme. A difference between the two estimates of the diabatic forcing, which is called the budget residual, indicates imbalances between the adiabatic and diabatic processes in the model. From the model integration the budget residual can be obtained by adding the monthly mean adiabatic and diabatic tendencies for a prognostic variable or simply by averaging the total initial tendency of the model over a month and subtracting the observed tendency (*Klinker and Sardeshmukh*, 1992). Here the initial tendencies are calculated from the difference between the first and second hour of the forecast in order to avoid some special features of the first time step.

The adiabatic tendencies (Fig. 3a) exhibit the warming due to large scale subsidence with maximum values of up to 2.8 degrees close to the boundary layer inversion and cooling in the lower part of the boundary layer. The diabatic tendencies produced by the parmetrization schemes (Fig. 3b) shows roughly a similar picture with opposite sign. However, there are quite large differences in magnitude. Therefore the sum of the adiabatic and diabatic tendencies has a significant residual (Fig. 3c), particularly close to the boundary layer inversion. Here the negative budget residual coincides with strong radiative cooling and further cooling due to evaporation in the shallow convection. Above the boundary layer inversion the radiative cooling seems to be insufficient to balance the adiabatic heating of the subsidence area. The budget residual of temperature corresponds to similar differences between first guess temperatures and sonde observations as shown in figure 1.

In Fig. 4 vertical profiles of diabatic processes are displayed as departures from the monthly mean sounding, where the departures have been calculated from an hourly tendency scaled to a 24 hour tendency. The same figure shows monthly mean profiles of vertical velocity , cloud cover and horizontal winds as well. For the location of this profile the most southern point of the ASTEX triangular has been chosen. The indication in these profiles, that a budget residual caused by large imbalances between adiabatic warming and radiative cooling in the cloud layer, suggests a problem in the cloud-radiation interaction. Too large cooling rates could arise from errors of cloud properties like too high cloud cover or from clouds which are optically too thick. It is hoped that cloud observations collected during ASTEX will help to determine the correct

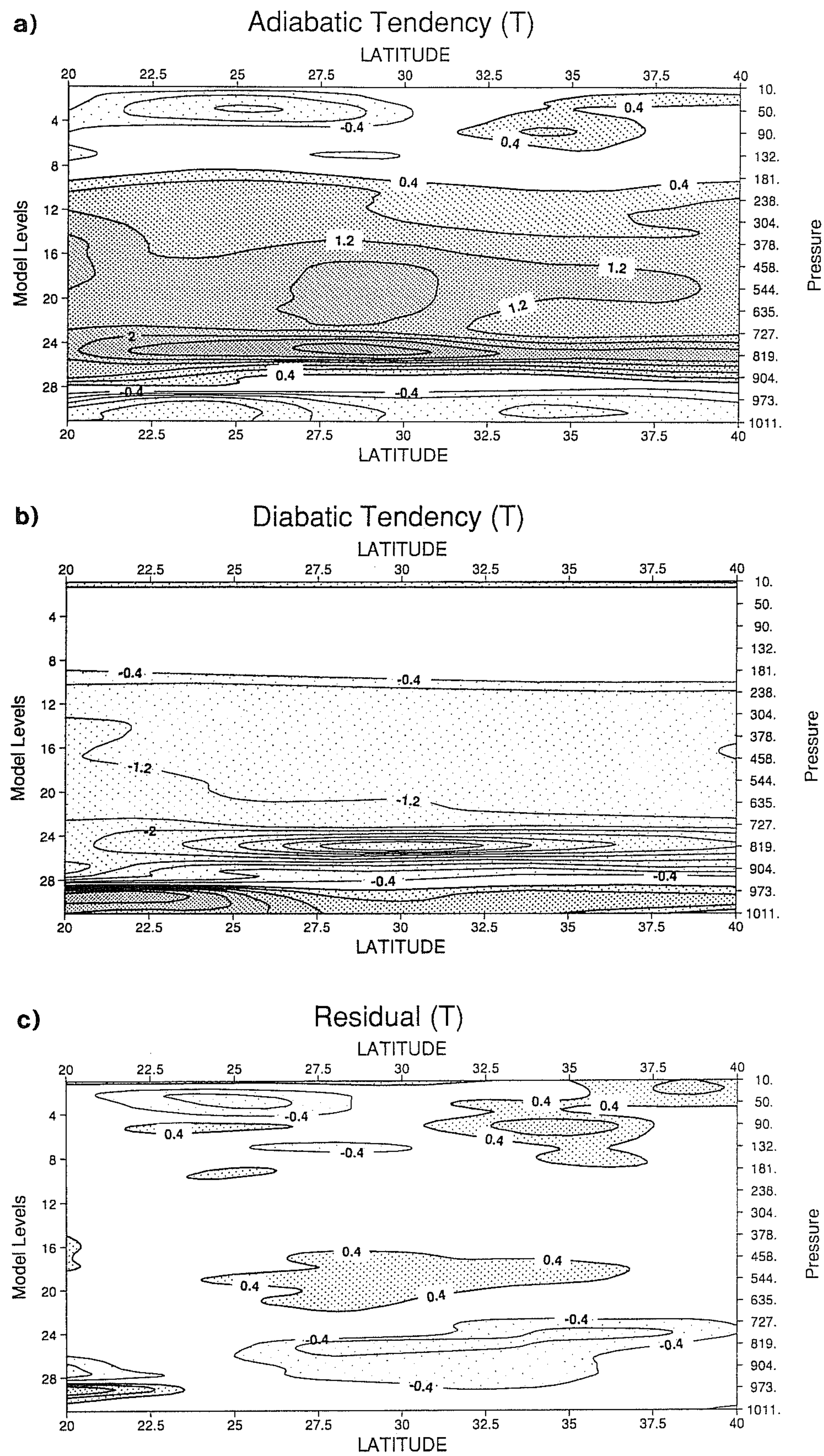

Fig. 3: Vertical cross section of the temperature budget for June 1992. Zonal mean from 25°W to 15°W. All tendencies are monthly averages calculated from the first and second hour of forecasts that were run four times per day. (a) adiabatic tendencies, (b) diabatic tendencies, (c) residual (a+b), (d) radiation, (e) cumulus condensation, (f) vertical diffusion. Units: K/day.

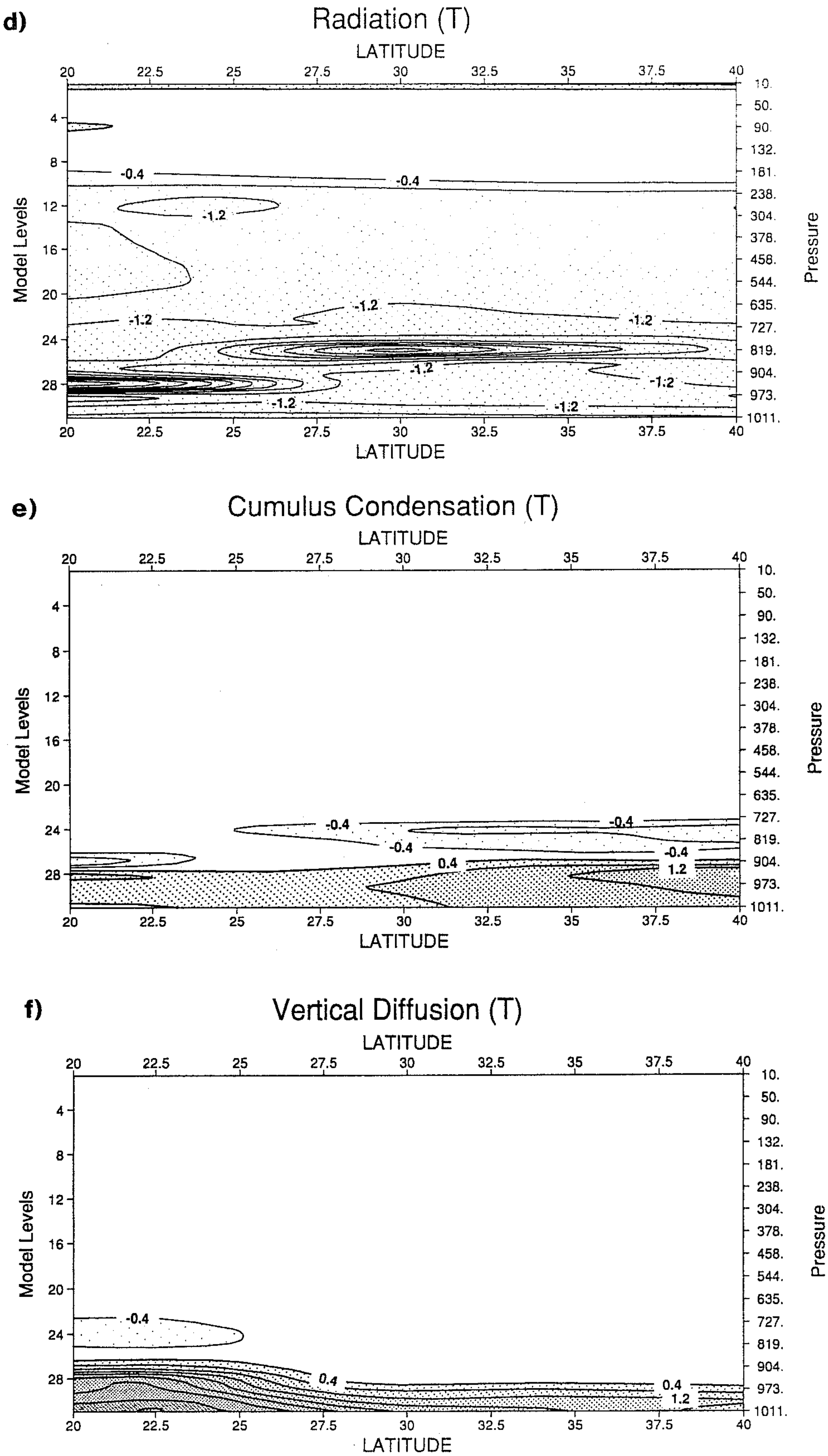

Fig. 3: continued

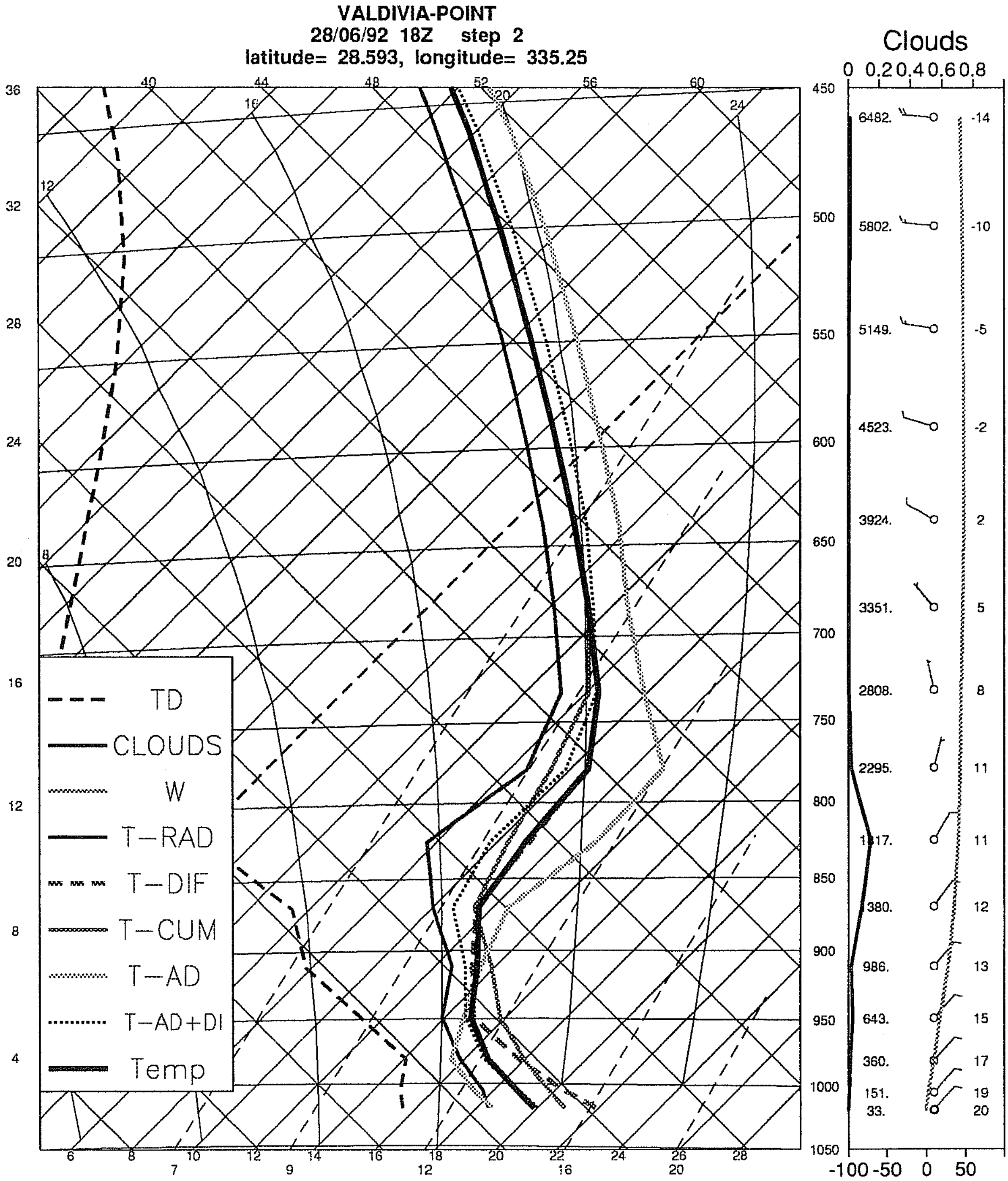

Fig. 4: Tehpigram of monthly mean temperature and dewpoint (left panel), cloud cover and average vertical velocity (right panel) for June 1992 at the most southern point of the ASTEX triangle. 24-hour diabatic tendencies are extrapolated from 1-hour tendencies (hour-2 minus hour-1 of the forecast) and drawn as deviation from the sounding of the analyzed temperature. The following tendencies are drawn: radiation (T-RAD), vertical diffusion (T-DIF), cumulus convection (T-CUM), adiabatic tendency (T-AD), and the sum of adiabatic and diabatic tendencies (T-AD+DI).

cloud forcing. Measurements of cloud properties and net radiation fluxes below and above the boundary layer inversion are required for a model validation.

The humidity budget (Fig. 5) is mainly controlled by vertical diffusion and shallow convection. The combined effect of both processes has the tendency to increase the specific humidity in the boundary layer which has to be compensated by advection of drier air. The imbalance between adiabatic and diabatic tendencies indicates an erroneous drying at the boundary layer inversion and just above. At the same time the model seems to produce an excessive moistening of the near surface layers. Assuming that errors of the adiabatic tendencies are comparatively small, then either the surface moisture flux is too large or the shallow convection is not efficient enough to transport moisture from near surface layers upwards into higher levels of the boundary layer.

Surface fluxes are difficult to validate due to a lack of observational data. It is hoped that measurements made during ASTEX will become available. First results from the research ship Le Suroit (private communication with *A. Weill*, CRNET, France) suggest monthly mean latent heat fluxes close to 100 Watts/m^2 and much smaller monthly mean sensible heat flux close to 10 Watts/m^2. The monthly mean surface flux of latent heat of the 24-hour forecast from ECMWF (Fig. 6) shows a distinct north-south gradient in the ASTEX area. Increasing values going south correspond to increasing sea surface temperatures and drier air. In the area close to Santa Maria, where the Le Suroit was cruising during June 1992 the ECMWF model fluxes of latent heat are just above 60 Watts/m^2. A more detailed comparison is, however, necessary to validate the model fluxes against observations.

4.1 Systematic temperature and humidity errors

The discussion of the budget residual was based on the very short range forecast. The results obtained there gain even more weight when they are still valid for a longer forecast range. In Fig. 7 cross sections of the forecast errors of day-1 and day-5 are shown for the same area as for the budget residual (Fig. 3). Though the magnitude of the budget residual seems to be an overestimate of the day-1 error, the vertical structure supports the link between negative temperature errors and the imbalance of radiative cooling and adiabatic warming close to the

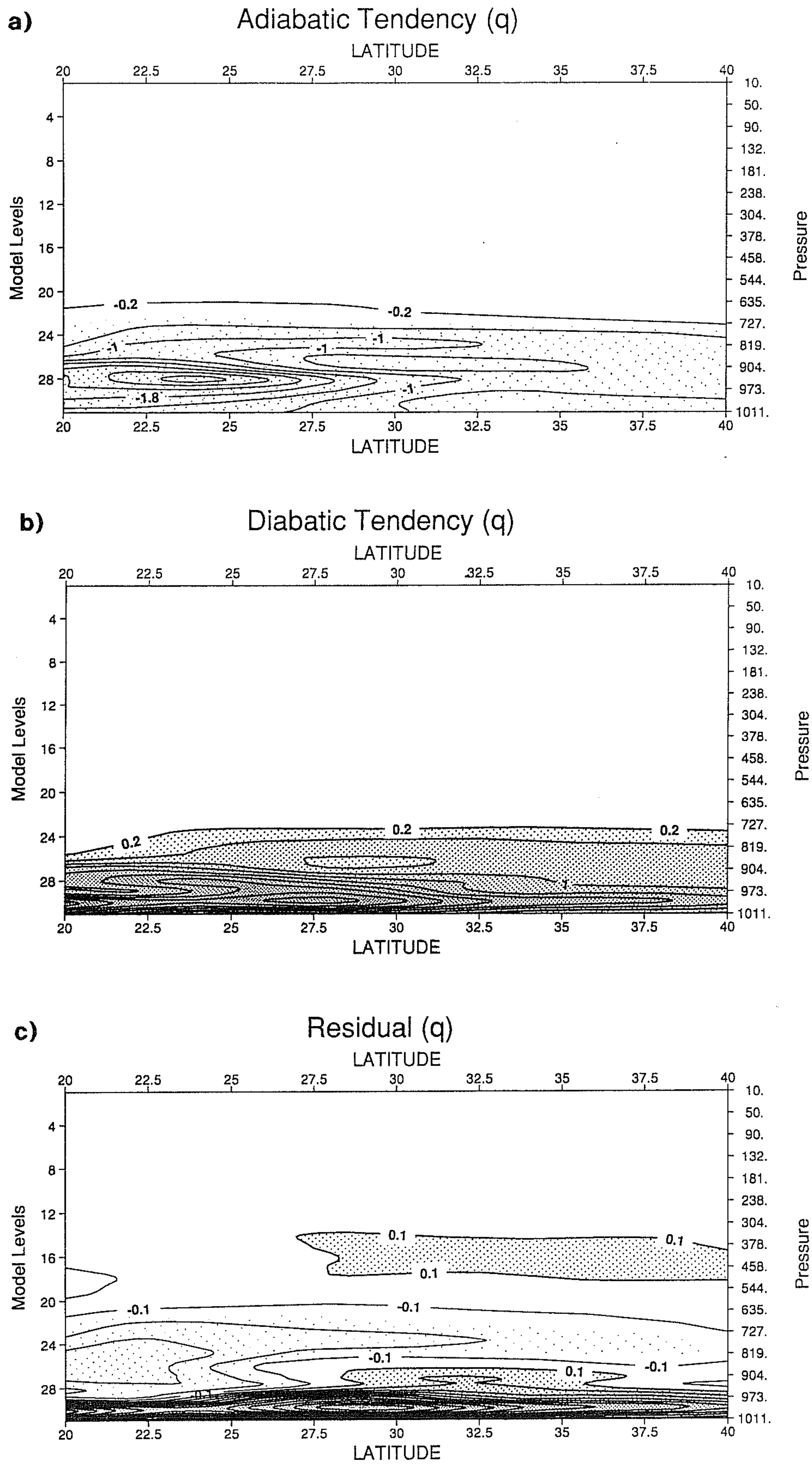

Fig. 5: Vertical cross section of the specific humidity budget for June 1992. Zonal mean from 25°W to 15°W. All tendencies are monthly averages calculated from the first and second hour of forecasts that were run four times per day. (a) adiabatic tendencies, (b) diabatic tendencies, (c) residual (a+b), (d) cumulus condensation, (e) vertical diffusion. g/kg/day.

d)

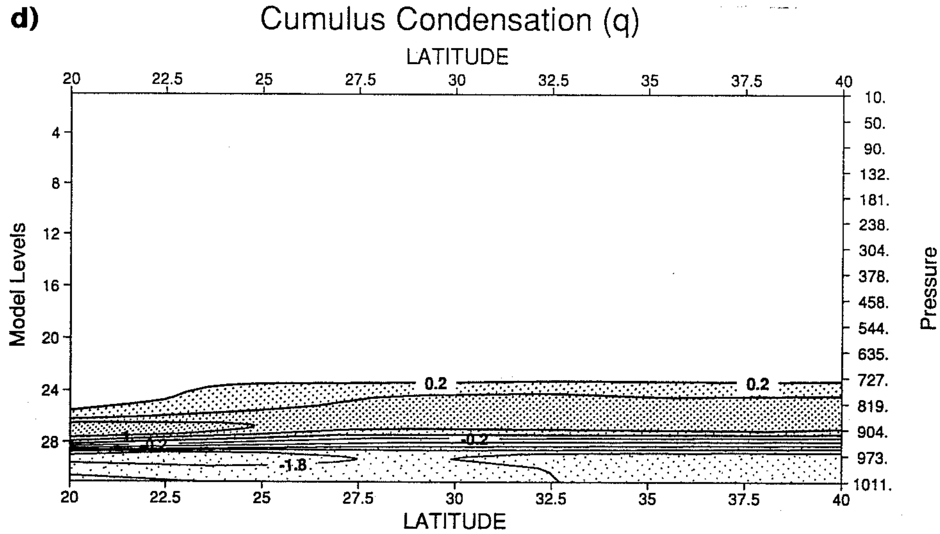

e)

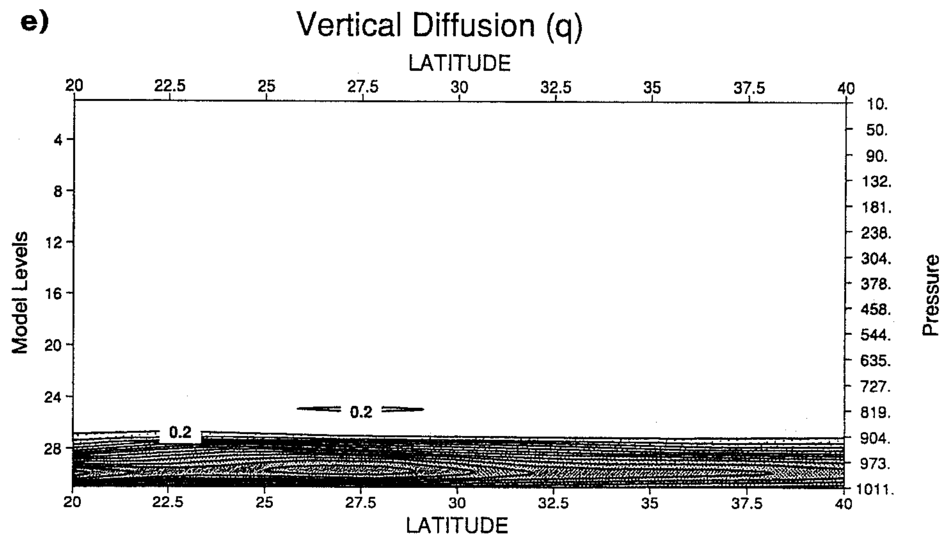

Fig. 5: continued

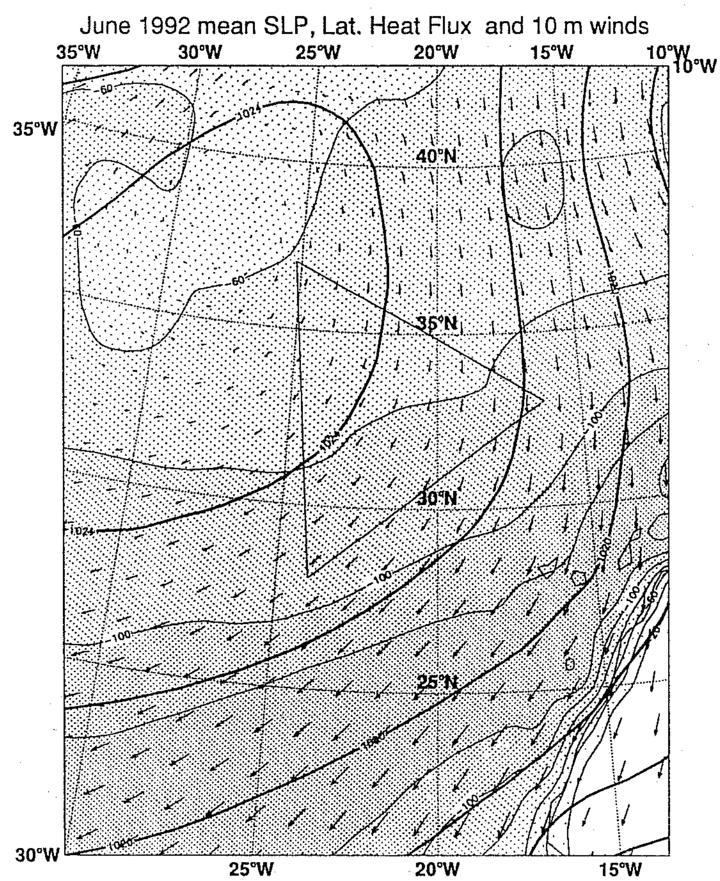

Fig. 6: Map of monthly mean sea level pressure (hPa) for June 1992, surface latent heat flux (Watts/m^2) and 10m winds (m/s) for June 1992 (24-hour forecast values).

a) Day-1 Temperature Error 9206

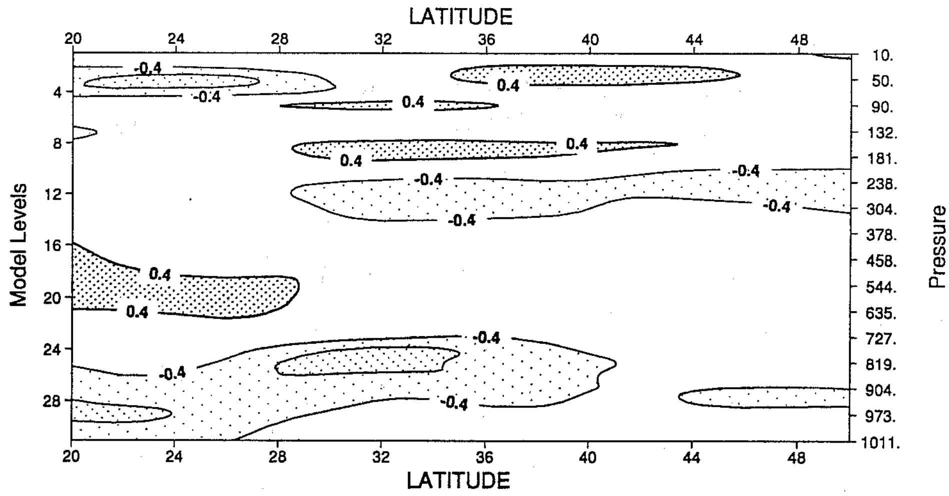

b) Day-5 Temperature Error 9206

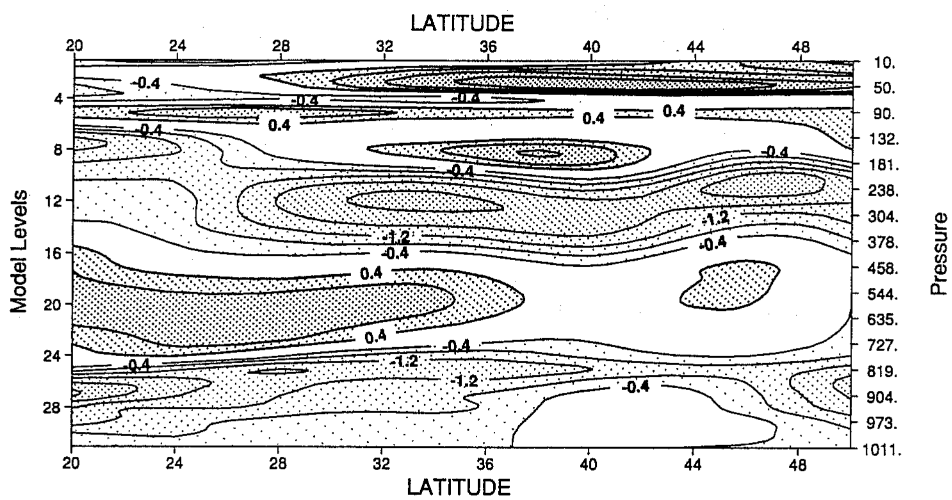

Fig. 7: Vertical cross section of monthly mean forecast errors of temperatures for June 1992, day-1 (a) and day-5 (b). Zonal mean from 25°W to 15°W. Units: K.

inversion. At a forecast range of 5 days this error structure has not changed very much, only the magnitude has increased. A negative temperature error is still a dominant feature of the upper boundary layer. Further up above the inversion positive temperature errors at day-5 correspond again to a budget residual of the same sign.

The budget analysis suggested that temperature errors are connected to problems with the cloud-radiation interaction. The could amount is difficult to verify against ISCCP data as middle and high level clouds are observed in the same area which can at times obscure low level clouds. Consequently the ISCCP clouds represent only a lower limit of low level cloud cover. A further problem is that simultaneous cloud observations were not yet available for June 1992. Therefore the model validation is done by comparing ISCCP clouds (Fig. 8) from several years with model clouds for June 1992 (Fig. 9) . The horizontal distribution of clouds in the model for June 1992 is characterized by a maximum just north of the Canary Islands. The variation of low cloudiness in the ISSCP data suggests that the low level cloud amount in the model is more likely to represent an underestimation. This would imply that temperature errors at the inversion level are presumably caused by problems of cloud optical properties rather than by an overestimate of cloud cover. The ISCCP observations also suggest that the maximum cloud cover in the model is too much to the South and to the South-West.

In the forecast the cloud amount in the ASTEX area is progressively increasing between day-1 and day-5 of the forecast. The cloud-radiation interaction on these slowly south-westward drifting clouds is strong enough to produce an increasing temperature error in the forecast (Fig. 10). At day-1 the negative temperature errors are found northwest of the Canary Islands. Further in the forecast the negative temperature errors increase and follow the south-west movement of the low level clouds.

The development of humidity errors during the forecast up to day-5 shows again some similarities to the budget residual of humidity (Fig. 11). Particularly the low level moistening and the drying in some parts of the upper boundary layer is a common feature of the two forecast ranges shown. However, at latitudes north of 38 degrees north, the moistening error in the day-5 forecast has penetrated into most parts of the troposphere.

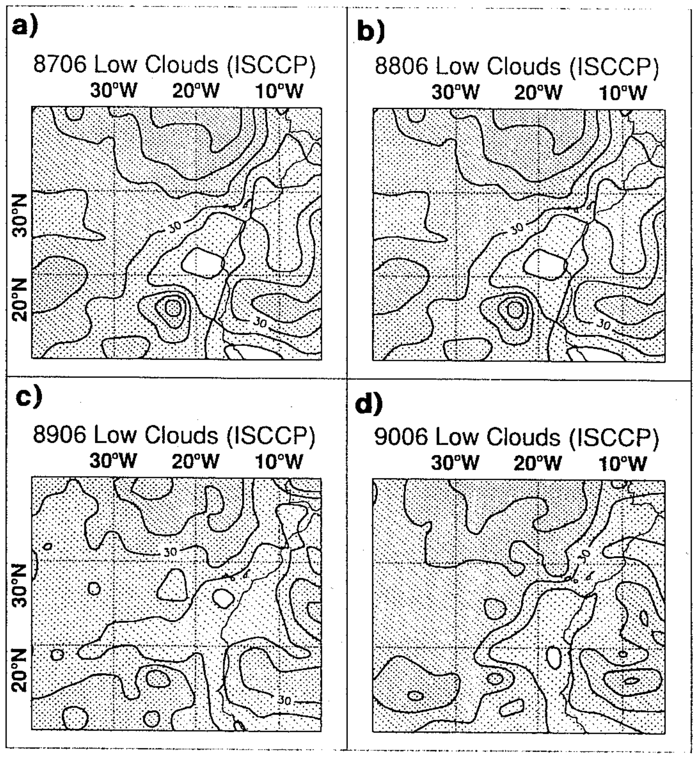

Fig. 8: June mean low level clouds from satellite retrievals (ISCCP). 1987 (a), 1988 (b), 1989 (c), 1990 (d).

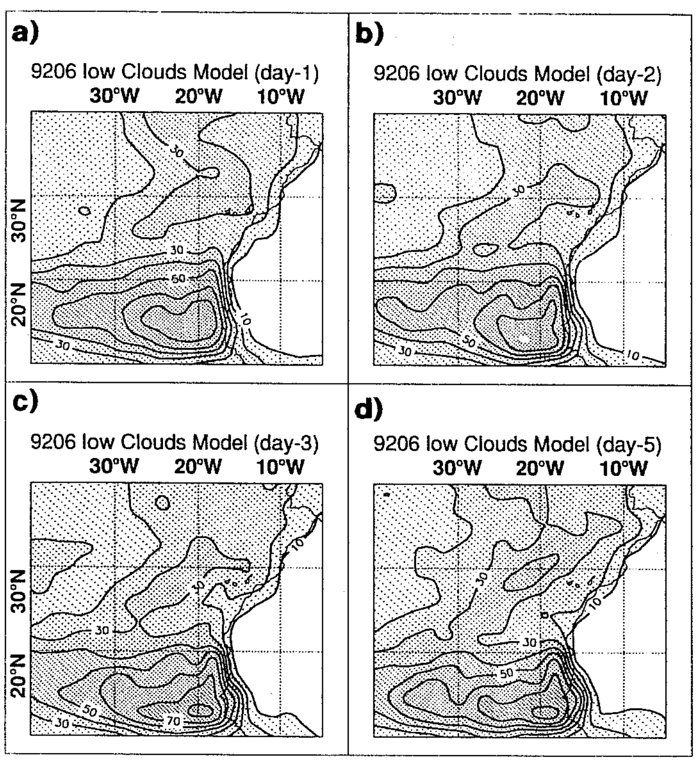

Fig. 9: June 1992 mean model low level clouds for forecast steps 24 hours (a), 48 hours (b), 72 hours (c), and 120 hours (d).

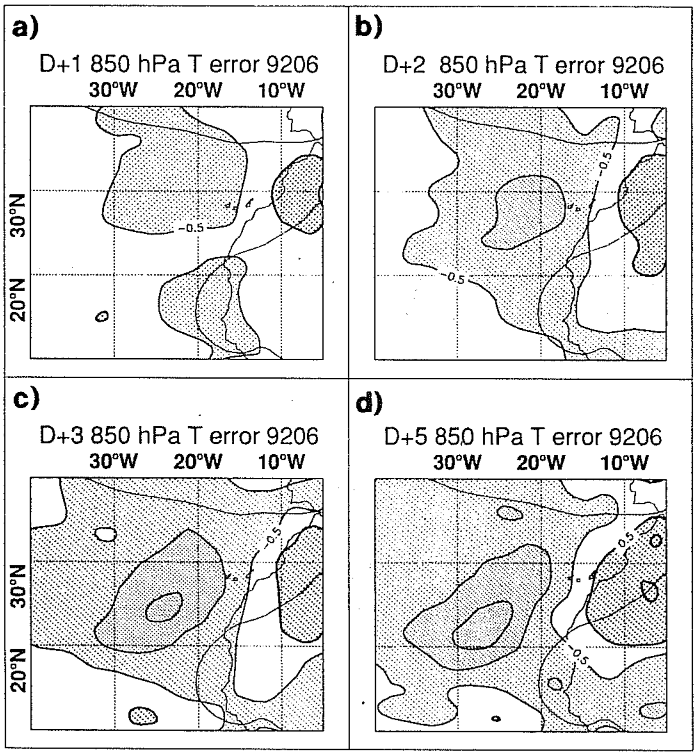

Fig. 10: June 1992 mean forecast temperature errors at 850 hPa for forecast steps 24 hours (a), 48 hours (b), 72 hours (c), and 120 hours (d). Units: K.

a) Day-1 Humidity Error 9206

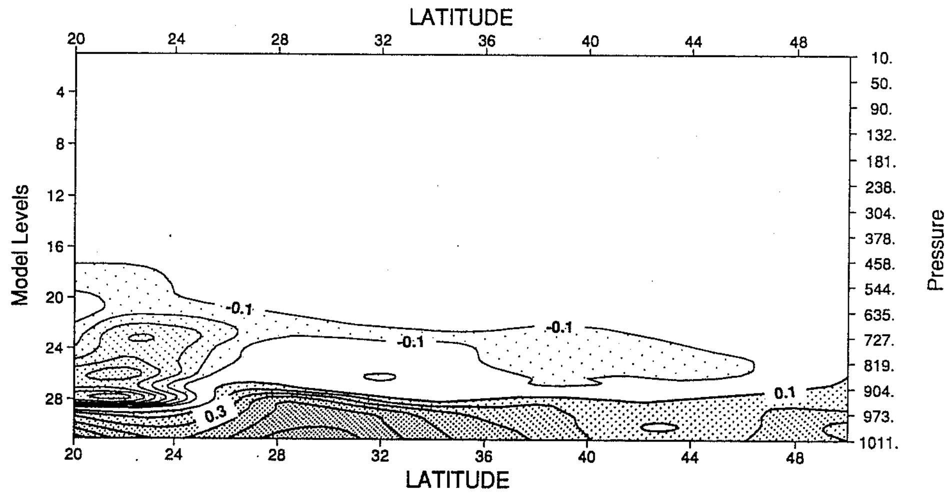

b) Day-5 Humidity Error 9206

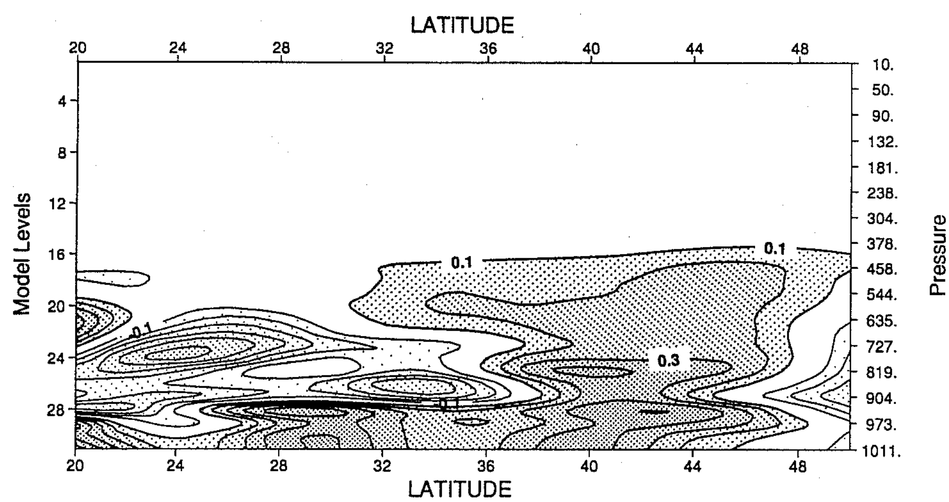

Fig. 11: Vertical cross section of monthly mean forecast errors of specific humidity for June 1992, day-1 (a) and day-2 (b). Zonal mean from 25^{0}W to 15^{0}W. Units: g/kg.

5. Summary

The ASTEX experiment has provided a large number of observations which have been distributed via the GTS and which have been successfully processed in the ECMWF data assimilation system. The additional radiosonde soundings used in the operational analysis were in the order of 100 for each analysis time, 0Z and 12 Z, and 70 for 6Z and 18Z. Improvements in the analysis were mainly seen in the error statistics of temperature.

The budget analysis of temperature and humidity suggested a link between systematic model errors and the diabatic forcing produced by the model's parametrization scheme. The model f ails to achieve a long term balance between the adiabatic warming and radiative cooling close to the inversion of the cloud topped planetary boundary. As the comparison of cloud cover with ISCCP clouds suggests a most likely underestimation of low level clouds in the model, the suggestion of excessive radiative cooling rates would have to be explained by errors in the cloud optical properties. Further improvements in the diagnostic cloud scheme are difficult to achieve, therefore a more physically based prognostic cloud scheme is now developed at ECMWF. It is hoped that a detailed validation of cloud cover and the structure of the boundary layer is possible with the complete set of ASTEX observations. Bulk measurements of radiation fluxes above and below the boundary layer clouds are required to validate the model's radiation scheme.

6. References

Klinker, E. and P. Sardeshmukh, 1992: the diagnosis of mechanical dissipation in the atmosphere from large_scale balance requirements. *J.Atmos.Sci.*, 49, 608-627.

Rossow, W.B. and R.A. Schiffer, 1991: ISCCP cloud data products. *Bull.Amer.Meteor.Sco.*, 72, 2-20.

Slingo, J.M. 1987: The development and verification of a cloud prediction scheme for the ECMWF model. *Quart. J. Roy. Meteor. Soc.*, 113, 899-927.

Tiedke, M. 1993: Representation of clouds in large-scale models. *Mon. Wea. Rev.*, 121, 3040-3061.